2012 IEEE International Conference on Robotics and Automation
RiverCentre, Saint Paul, Minnesota, USA
May 14-18, 2012

Metal MEMS Tools for Beating-heart Tissue Removal

Andrew H. Gosline, *Member, IEEE*, Nikolay V. Vasilyev, Arun Veeramani, MingTing Wu, Greg Schmitz, Rich Chen, Veaceslav Arabagi, *Member, IEEE*, Pedro J. del Nido and Pierre E. Dupont, *Fellow, IEEE*

***Abstract*— A novel robotic tool is proposed to enable the surgical removal of tissue from inside the beating heart. The tool is manufactured using a unique metal MEMS process that provides the means to fabricate fully assembled devices that incorporate micron-scale features in a millimeter scale tool. The tool is integrated with a steerable curved concentric tube robot that can enter the heart through the vasculature. Incorporating both irrigation and aspiration, the tissue removal system is capable of extracting substantial amounts of tissue under teleoperated control by first morselizing it and then transporting the debris out of the heart through the lumen of the robot. Tool design and robotic integration are described and ex vivo experimental results are presented.**

I. INTRODUCTION

Surgical robotic systems are gaining popularity in clinical practice due to benefits such as motion scaling, tremor cancellation, enhanced or augmented displays, improved dexterity, and improved access to the surgical site. Often, and perhaps most significantly, the goal of these surgical robots is to convert procedures that are typically done in an open fashion to a minimally invasive fashion. In the specific case of cardiac procedures performed inside the heart, minimally invasive surgery eliminates the need to cut open the chest (sternotomy). More importantly, if these procedures can be performed while the heart is beating (avoiding cardiopulmonary bypass), there is substantial benefit to the patient in terms of reduced neurological risks.

While the introduction of catheters has transformed the treatment of simple repairs by enabling beating-heart access through the vasculature, many procedures remain possible only by open surgery on the stopped heart. There are several reasons for this. Despite recent advances in catheter technology [1], [2], [3], [4], [5], they can neither apply enough force to the tissue, nor be positioned accurately enough for complex surgical repairs.

Furthermore, appropriate tools do not exist for performing the surgical tasks of tissue removal and tissue approximation inside the beating heart. While for many applications, it is possible to develop robots that use existing surgical tools to perform procedures in a manner comparable to manual surgery techniques, such as bronchial endoscopy [6] and laparoscopy [7], the environment of the beating-heart precludes this approach. First, the chambers of the heart are too small to perform complex manipulations of tools. Secondly, tool manipulations cannot interfere with operation of the heart, for example, by occluding blood flow or by inducing arrhythmias. Thirdly, the procedure is performed in the bloodstream where high magnitude and varying flow velocities make tool control and visualization difficult.

Prior work by our group has considered the design of a robotically-delivered tissue approximation device for percutaneous beating-heart closure of a PFO [8]. The device has been recently validated with in vivo porcine experiments. This work provided a novel alternative to both catheter-delivered occlusion devices and to surgical closure by suture.

This paper considers the task of tissue removal inside the beating heart. In contrast to tissue approximation, no catheter-based alternative to open surgery is available for removing tissue inside the heart. Tissue removal is an important component of many intracardiac procedures and is applicable to both the pediatric and adult populations.

In the treatment of congenital heart disease, for example, the outflow tract of either ventricle may be obstructed by excess muscle tissue. Figure 1(a) illustrates the abnormally formed muscle shelves that can obstruct flow leaving the right ventricle through the pulmonary valve. Figure 1(b) illustrates the comparable situation of an aortic valve obstruction in the left ventricle. Either procedure can involve removing several cubic centimeters of tissue.

As a final example, adults can suffer from thickening and calcification of the aortic valve leaflets as shown in Figure 1(d). The thickened leaflets are not as flexible as healthy leaflets and consequently fail to open and close completely resulting increasing the load on the heart. Surgically, this condition is repaired by thinning the leaflets at their base.

The contribution of this paper is a robotically controlled, steerable tissue removal device for intracardiac surgery. A concentric tube robot platform is used to deliver a novel metal MEMS tissue removal tool. As a demonstration procedure, tissue removal from the outflow tract of the pulmonary valve is considered. As shown in Figure 2, the robot enters the heart percutaneously from the right internal jugular vein and passes through the tricuspid valve into the right ventricle.

From there, the robot can be navigated to the outflow tract of the pulmonary valve and the cutting tool can be employed to sculpt away excess tissue. The cutting tool provides integrated irrigation and aspiration so that the morselized debris can be transported out of the heart through the lumen of the robot. Irrigation using heparized saline facilitates transport

This work was supported by the National Institutes of Health under grants R01HL073647 and R01HL087797.

A. Gosline, N. Vasilyev, V. Arabagi, P. del Nido, P. Dupont are with Cardiovascular Surgery, Children's Hospital Boston, Harvard Medical School, Boston, MA, 02115, USA. {Andrew.Gosline, Nikolay.Vasilyev, Veaceslav.Arabagi, Pedro.DelNido, Pierre.Dupont}@childrens.harvard.edu

A. Veeramani, M. Wu, G. Schmitz and R. Chen are with Microfabrica Inc., Van Nuys, CA, USA

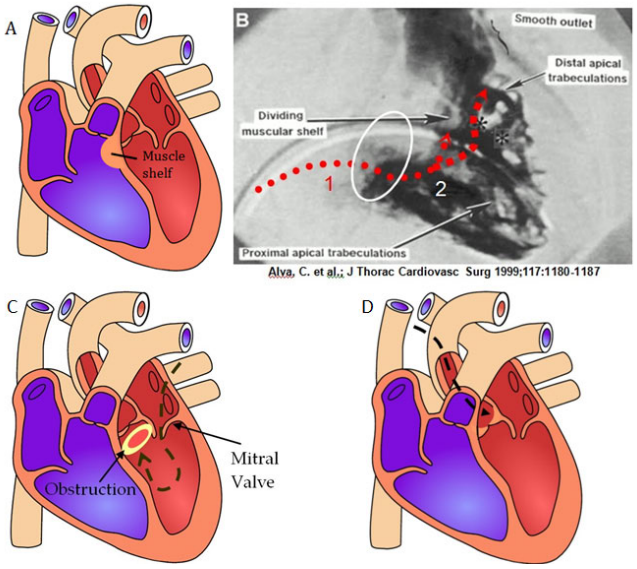

Fig. 1. Cardiac conditions requiring requiring tissue removal by open surgery on a stopped heart: (a) obstruction of the pulmonary valve outflow tract, (b) angiogram image of obstructing tissue, (c) obstruction of the aortic valve outflow tract, (d) thickened aortic valve leaflets impeding normal valve function.

while minimizing both blood loss and device clogging due to emboli formation.

Concentric tube robots are a relatively new class of continuum robots that consist of pre-curved elastic tubes in a telescoping arrangement. Active shape change is achieved by relative rotation and translation of the tubes at their base. Concentric tube robots are capable of navigating vasculature, similar to catheters, but offer substantially higher force output and position accuracy [9], [10], [11], [12]

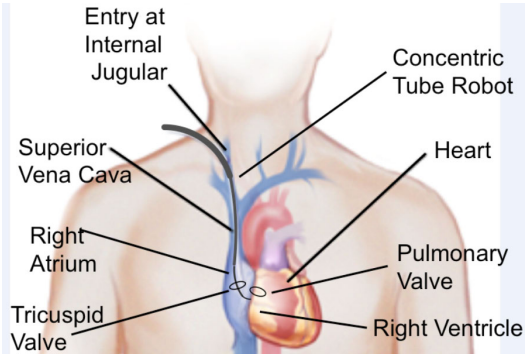

Fig. 2. Concentric tube robot entering the beating heart via the internal jugular vein.

The paper is arranged as follows. The next section describes the metal MEMS manufacturing techology used to fabricate the device. The following section describes the surgical requirements and design of the device. Next, integration of the cutting tool with a concentric tube robot is detailed. Ex vivo experiments are then described followed by conclusions and a description of future work.

II. Metal MEMS Fabrication Technology

Presently, millimeter scale surgical devices are manufactured in metal using conventional methods such as computer-numerically controlled (CNC) machining, electrical discharge machining (EDM), laser cutting, or grinding. Additionally, much of the micro electro mechanical (MEMS) research involves creating components out of silicon wafers using techniques that were adopted from solid state electronics and microchip manufacturing. These available technologies have significant limitations when it comes to making functional assemblies of moving parts at the millimeter scale that have to perform surgical functions such as approximate or remove tissue. Silicon is a brittle material, and conventionally machined metal parts are difficult, inaccurate, or expensive to assemble.

Unlike prior art, the MEMS technology used here (Microfabrica Inc, Van Nuys, CA) is an additive, lithography EFAB (Electrochemical FABrication) based manufacturing process that can create intricate 3D shapes with moving parts without assembly. The process is based on depositing successive layers of a structural material (NiCo in this case) and a sacrificial one (Cu), thus building any part from the ground-up, as illustrated in Fig. 3. The presence of a sacrificial layer allows for creation of overhangs, bearing surfaces, and multi-part assemblies all in one manufacturing step. The parts are released in the final step of the process by etching away the sacrificial material.

Given that the method relies on selectively electroplating the structural material, its layers feature excellent adhesion, with the final manufactured parts exhibiting structural properties similar to those of a monolithic material [13]. Thus, the process allows designers to transform complex assemblies with moving parts, hinges, bearings, and threads with feature sizes of a few microns directly from CAD renderings to metal parts. Finally, given that the EFAB process is a batch manufacturing technique, it allows large volume production of parts all at once at low cost. The MEMS EFAB process has been previously used by our group to create a tissue approximation device for patent forman ovale closure [8].

III. Device Design

Standard techniques for surgically removing tissue inside the heart include the use of scalpel, forceps and scissors to retract, cut and remove the desired tissue. Since the heart is stopped, tissue debris can be manually removed as well as flushed from the heart chambers without risk of debris escaping into the bloodstream where it could create emboli.

Recreating the full range of tissue removal techniques that an experienced surgeon can accomplish with hand tools is extremely challenging for a robotic system. An appropriate strategy for designing a robotic tissue removal tool, however, is to consider the requirements of the tissue removal tasks as well as the constraints imposed by the surgical environment and those of the robotic delivery system. In this way, the tool design requirements can be grouped as surgical requirements and robot delivery requirements.

Surgical requirements:

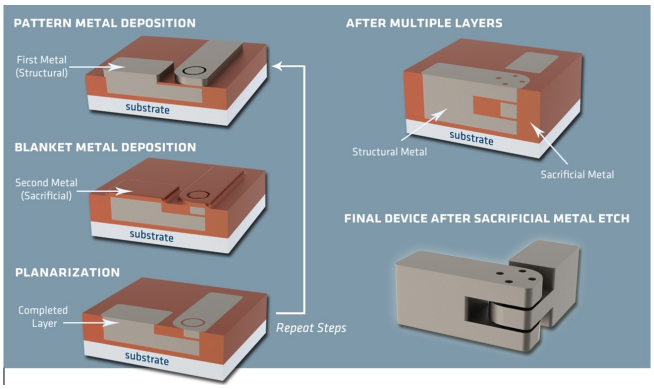

Fig. 3. Metal MEMS fabrication process - revolute joint example. The formation of each layer involves three steps: (a) pattern deposition of a structural metal, (b) blanket deposition of sacrificial metal, and (c) planarization. After all layers are formed, the sacrificial metal is removed, leaving behind the assembled 3D device.

1) Tissue to be removed may consist of only thin surface layers or may form thick muscular layers.
2) Tool must effectively cut (without excessive tearing) endocardial tissue layer which is extremely strong and elastic.
3) Tissue debris cannot escape into the blood stream if it is large enough to create emboli (diameter $>$ 50 microns).
4) Blood loss arising from aspiration should be limited.

Robotic delivery requirements:

1) Tool / robot diameter is limited to 3 mm to enable percutaneous delivery through the vasculature in children and adults (8 mm diameter catheters have been used for adult aortic valve replacement).
2) Cutting tool power must be delivered through the robot as its curvature and length varies.
3) Morselized tissue must also be evacuated through the lumen of the robot without becoming jammed in either tool or lumen.

Together these requirements can be combined to produce a set of tool design requirements as described below.

Functional design requirements:

1) Tool must be capable of cutting tissue at its tip in order to enable removal of thick muscular layers.
2) To provide precise control for the removal of surface layers, tool should have a cutting guard that prevents undesired deep cutting as a result of cardiac cycle motion.
3) The tool design should be scalable in diameter in order to provide the means to trade off tissue removal precision with removal rate.
4) To ensure entrainment and transport of tissue debris while minimizing blood loss, tool should provide integrated irrigation as well as aspiration.

No existing medical devices meet these functional requirements. While there are biopsy catheters, they are only capable of taking small bites of tissue and so cannot be used effectively for either the removal of surface layers or the removal of bulk tissue. Existing powered instruments for the mechanical removal of tissue are typically too large and are designed as a pair of concentric closed rotating tubes with a cutting window on the side. Tissue removal depends on the herniation of tissue into the window - a design which has limited effectiveness at small diameters and for smooth tissue surfaces. Furthermore, since the cutting window is located on the side of the tip of the tool, they are incapable of performing plunge cuts or sculpting the tissue to create a desired surface profile. Thus, a completely new tissue removal technology is needed to meet the functional requirements.

A. Design Features

Unlike the machining of stiff materials such as bone and metal, a cutting device for soft tissue cannot rely on the reaction force of the tissue to generate sufficient force for cutting. Furthermore, capture of debris necessitates a cutting action in which the tissue "chips" that are generated are entrained in a flow leading into the cutter head and not the bloodstream. These requirements suggest a stator / rotor tool geometry for producing a scissoring action on the tissue.

We have produced many different cutting tools of this type, one of which is depicted in Figure 4. The light gray component acts as the stator and is fixed to the distal tube of the robot. It includes two large cutting windows 180 degrees apart. The rotor, shown in dark gray, rotates relative to the stator and possesses two sets of five sharp cutting teeth that grab any tissue projecting into the cutting windows of the stator.

The sharp leading edges of the stator and the rotor enable the device to grab and slice the tough endocardial tissue layer. The multiple sets of interlocking teeth in each window ensure that the entrained tissue is cut into smaller pieces. Ideally, morsel size should be about $1/10$th the diameter of aspiration lumen to aid transport and minimize the potential of clogging. The number of teeth are selected to balance this desired bite size with mechanical strength of the cutting components.

Even though the tool will not be operating while it is being navigated over the surface of the beating heart to the surgical site, it is important to provide the means for avoiding accidental tissue damage that could occur if the sharp edges of the tool dig into the tissue. To prevent this, the outer portions of the stator that are not cutting windows function as cutting guard surfaces. When the tool is drawn across tissue such that the stator guards are in contact, the tissue is protected from these sharp edges - even when the tool is operating. To perform cutting, the tool must be turned on and moved so as to direct tissue into the cutting windows.

Since the MEMS fabrication process used to create these tools builds the devices from thin planar layers, device cost and complexity is closely tied to the number of layers. An advantage of the rotor-stator design is that its diameter can be easily scaled, e.g., from 1-5 mm, using approximately the same number of layers. The depicted version has a diameter of 1.8 mm and was fabricated from 36 layers,

each 25 microns thick. The number of mating cutting teeth can be scaled with diameter to control bite size, although the larger diameters aspiration lumens are also capable of accommodating larger debris.

As shown in Figure 5, the rotor is driven using a rotating tubular drive element with a suction source connected to its lumen at the proximal end. A small gap between the drive tube and the innermost (distal) robot tube is used to pump heparinized saline into the chamber between the rotor and stator. This irrigating flow serves to transport debris through the aspiration lumen with minimal blood loss while its heparine prevents the formation of emboli inside the device and aspiration lumen.

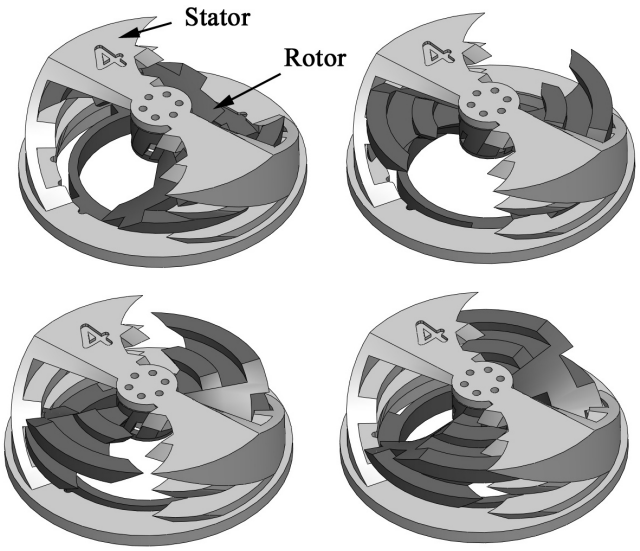

Fig. 4. Tissue removal tool design depicted at four angles of rotation.

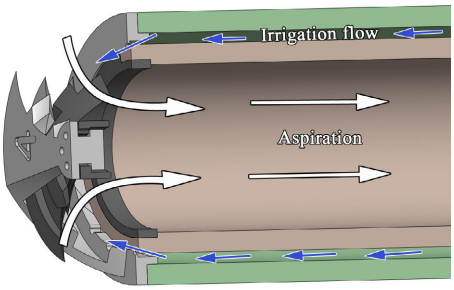

Fig. 5. Cutaway view of the tissue removal tool to illustrate fluid flow. The outer annular channel supplies heparinized saline while the inner channel provides aspiration to remove debris.

IV. Robot-tool Integration

Concentric tube robots, as shown in Figure 6, are comprised of pre-curved elastic tubes in a telescopic arrangement. Each tube can be translated, rotated, or both, relative to the other tubes to generate shape change. Each section along the length of the robot can have either a fixed or a variable curvature.

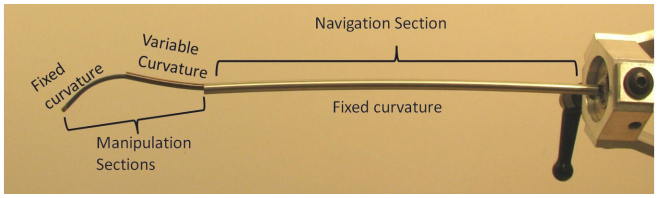

Fig. 6. Concentric tube robot for tissue removal.

Our group has previously developed optimization algorithms for the selection of tube parameters (lengths and curvatures) given a surgical task and anatomical constraints [14]. The method decomposes the concentric tube robot into sections that navigate to the surgical site, referred to as navigation sections, and sections that interact with the tissue at the surgical site, referred to as manipulation sections. Table I lists the tube parameters for the robot of Figure 6.

Section	Length (mm)	Radius of Curvature (mm)
1	200	800
2	45	80 to ∞
3	35	25

TABLE I
Concentric Tube Robot Design Parameters. Section numbers are from right to left in figure above.

A. Tool-robot Mounting

It is generally preferable to design tools for insertion and removal through the proximal end of the robot. This approach enables the robot to be held in position inside the body while a tool is changed and so avoid the need to remove the robot during replacement. This approach was utilized for the tissue approximation device reported in [8]. For high-speed rotating tools, however, this method is more challenging because tool control requires applying torques between two tubular elements. Mounting the tool from the distal end allows the use of a robot tube as one of the two control elements. Proximal-end loading would require two additional tubes to be loaded from the proximal end which would substantially increase the overall diameter. Furthermore, the cutting surfaces would need to be protected as they were inserted through the robot lumen to avoid dulling prior to use.

Consequently, it was decided to use a single drive tube and to insert the assembly from the distal end. To attach the tool assembly to the distal robot tube, an axially symmetric pattern of mating snap-in 'dog ears' was designed as shown in Figure 7(a,b). The pattern was laser cut in the NiTi robot tube. This design allows for axial and radial alignment, torque transmission, while ensuring easy and accurate assembly / dissassembly.

B. Drive System

The tool drive system was designed to attach to the proximal end of the robot drive stage controlling the distal

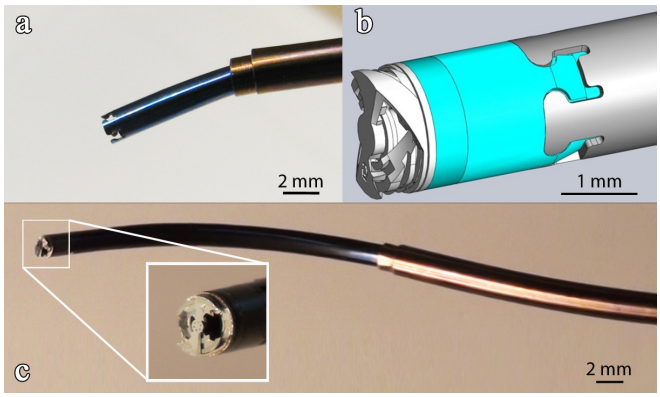

Fig. 7. Snap-in mounting system to connect tissue removal tool to the distal NiTi robot tube. (a) Robot showing laser cut dog ear pattern. (b) CAD model showing assembled tool and robot. (c) Actual assembly.

robot section. Since this section is constant curvature, it is comprised of a single tube driven by a 2 DOF stage (one rotation and one translation) that was designed to include a mounting flange and set screws to mate with the tool drive system. The inner drive tube of the tool passes through the entire length of the robot and is fastened to the tool drive system. Figure 8 illustrates the location of the tool drive as it is mounted in the concentric tube robotic drive sytem.

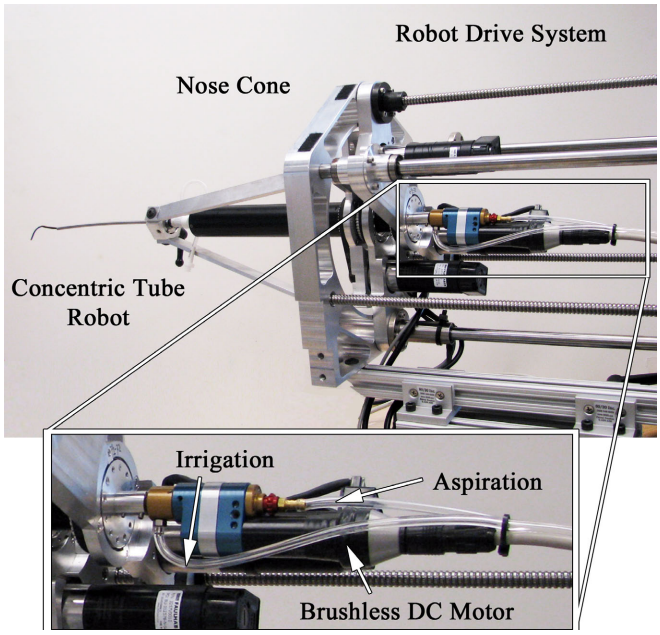

Fig. 8. Concentric tube robot showing tool drive mounted on distal section drive stage. Inset provides detail view.

A speed controlled tool drive was designed to deliver torque and provide aspiration and irrigation. Because the concentric tube robot changes its shape through active manipulation, and there is a finite clearance between each of the concentric tubes, the arc length of the robot varies slightly during use. To accommodate this axial play, a floating gearing system was designed to allow 3mm of axial motion without gear binding. The gear on the drive shaft is attached with a split collar (to facilitate loading from the distal end) and the shaft is supported by a bronze bushing and sealed bearing arrangement. High tolerance bronze bushings were pressed into sealed bearings so that the drive shaft can slip easily on the bushing axially, but transmits most of the rotational load to the bearings.

A brushless DC motor (Faulhaber, DE) with integrated hall effect sensors was chosen for the drive system because of its high torque, compact diameter, and speed control electronics. The motor is driven with a three phase, PWM motor driver (Faulhaber, DE) at 24VDC. The components of the tool drive are shown in Figure 9.

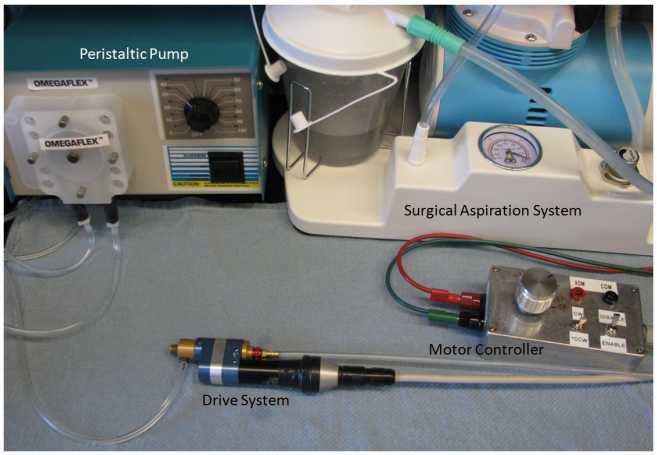

Fig. 9. Components of the tool drive system.

Irrigation requires that heparinized saline is delivered to the tool tip at a prescribed rate. A peristaltic pump is used for this purpose since the fluid is kept sealed from contamination as it travels through disposable, pre-sterilized tubing. A variable speed pump (OmegaFlex Inc.) provides a flow rate of 32ml/min - 200ml/min. A portable surgical aspiration system (Schucco Inc.) provides vacuum and debris capture. This device employs a reciprocating pump, and supplies negative pressure from 1 - 18 inHg to a 700cc canister.

V. Ex Vivo Experiments

Ex vivo experiments using porcine hearts were performed to develop a percutaneous procedure for the removal of obstructions in the outflow tract of the pulmonary valve. The proposed procedure involves entering the heart from the internal jugular and navigating into the right atrium from the superior vena cava. The robot navigates through the tricuspid valve by passing through a commissure to ensure that the valve can continue to operate during the procedure. Reaching the outflow tract of the pulmonary valve, the proximal navigation sections of the robot are then held fixed while the distal manipulation sections are teleoperated under ultrasound guidance to sweep the tissue removal tool over the excess tissue and thus remove it.

The experiment is shown in Figure 10. A supermarket-procured porcine heart was excised from the entry point at the superior vena cava, through the right atrium, the tricuspid

valve, and into the right ventricle to enable visualization of the robot and the progression of cutting. The heart was then immobilized by suturing it to an aluminum fixture. Finally, the heart and fixture were placed in an anatomically correct location with respect to the robot for entry at the jugular.

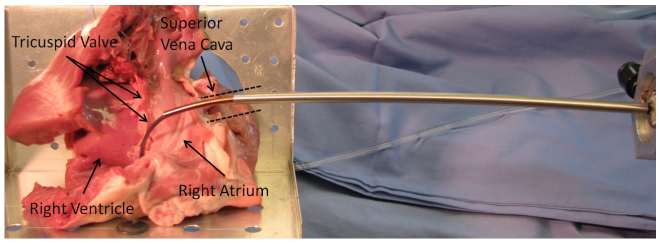

Fig. 10. Ex vivo experimental set up.

A. Selection of Cutting Parameters

Experimentally optimized values of rotation rate, irrigation flow, and aspiration pressure were obtained through testing different types of cardiac tissue prior to the ex vivo surgical experiments. Variation of the rotation rate has a considerable effect on the cutting behavior. High rotation speeds are very effective at removing a thin layer of endocardium, as shown in the upper portion of Figure 11. Slower speeds yield better results for removal of bulk material. For both settings, the aspiration and irrigation parameters were set to 15 inHg vacuum and 100 ml/min flow, respectively. At these settings, there is an accumulation of fluid on the cutting surface, but no visually observable tissue debris.

B. Cutting Results

Figure 11 shows results from the cutting experiments on two types of tissue. Near the top, removal of the endocardial surface layer was performed with a gentle sweeping motion along the surface, with the tool positioned at an angle of 45 degrees from normal Note that the underlying muscular tissue is exposed, and that the shiny, smooth endocardium has been removed in a roughly rectangular pattern. Lower down in the figure, a cavity was milled into the tissue by pressing the tool into the tissue with a normal approach and sweeping it in a small circular pattern to expose the surrounding tissue to the cutting windows of the tool.

While little cutting debris was visible on the tissue surface, a downstream embolization filter will be deployed in the main pulmonary artery in future in vivo experiments to collect any particulate emboli that may be dislodged by the process of tissue removal.

VI. Conclusions and Future Work

Successful application of robotics in surgery necessitates the creation of new approaches, techniques and tools. This paper provides such an approach to a previously unaddressed clinical need - removing tissue inside a beating heart. We have proposed and fabricated a solution that incorporates two promising novel technologies: metal MEMS tools and concentric tube robots. This robotic system provides a steerable yet stiff platform for controlling tool-tissue contact so as to enable precise tissue removal while also satisfying the stringent constraints of operating inside the beating heart. Toward our goal of in vivo testing, systematic studies are planned to evaluate tool tip stability and cutting accuracy on moving tissue and to further characterize the relationship between tool speed, feed rate, irrigation and aspiration as well as their effect on cutting performance.

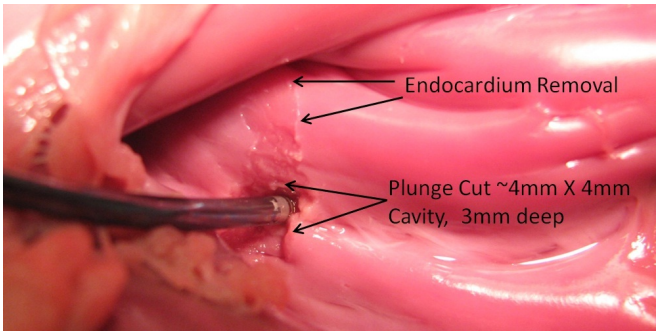

Fig. 11. Ex vivo robotic tissue removal near the outflow tract of the pulmonary valve. Illustrated cutting tasks include removal of endocardial surface layer and also bulk removal of myocardium.

References

[1] M. Ikeuchi and K. Ikuta, "Development of pressure-driven micro active catheter using membrane micro emboss following excimer laser ablation (MeME-X) process," in *IEEE Int. Conf. Robotics and Automation*, 2009, pp. 4358–4361.

[2] S. Kesner and R. D. Howe, "Design and control of motion compensation cardiac catheters," in *IEEE Int. Conf. Robotics and Automation*, 2010, pp. 1059 – 1065.

[3] D. Camarillo, C. Milne, C. Carlson, M. Zinn, and J. Salisbury, "Mechanics modeling of tendon-driven continuum manipulators," *IEEE Trans. Robot*, vol. 24, no. 6, pp. 1262–1273, 2008.

[4] D. Camarillo, C. Carlson, and J. Salisbury, "Configuration tracking for continuum manipulators with coupled tendon drive." *IEEE Trans. Robot*, vol. 25, no. 4, pp. 798–808, 2009.

[5] J. Jayender, R. V. Patel, and S. Nikumb, "Robot-assisted active catheter insertion: Algorithms and experiments," *Int J Robot Res*, vol. 28, no. 9, pp. 1101–1117, 2009.

[6] N. Simaan, K. Xu, A. Kapoor, W. Wei, P. Kazanzides, P. Flint, and R. Taylor, "A system for minimally invasive surgery in the throat and upper airways," *Int J Robot Res*, vol. 28, no. 9, pp. 1134–1153, 2009.

[7] A. Madhanir, G. Niemeyer, and J. Salisbury, "The black falcon: A teleoperated surgical instrument for minimally invasive surgery," in *IEEE/RSJ Int.l Conf. on Intelligent Robots and Systems*, 1998, pp. 936–944.

[8] E. Butler, C. Folk, A. Cohen, N. Vasilyev, R. Chen, P. del Nido, and P. Dupont, "Metal MEMS Tools for Beating-heart Tissue Approximation," in *IEEE Int. Conf. on Robotics and Automation*, 2011, pp. 411–416.

[9] P. Dupont, J.Lock, E. Butler, and B. Itkowitz, "Design and control of concentric tube robots," *IEEE Trans. Robot*, vol. 7, pp. 304–306, 2010.

[10] M. Mahvash and P. Dupont, "Stiffness control of continuum surgical manipulators," *IEEE Trans. Robot*, vol. 27, no. 2, pp. 334–345, 2011.

[11] J. Lock, G. Laing, M. Mahvash, and P. Dupont, "Quasistatic modeling of concentric tube robots with external loads," in *IEEE/RSJ Int. Conf. on Intelligent Robots and Systems*, 2010, pp. 2325–2332.

[12] D. Rucker, B. Jones, and R. Webster, "A geometrically exact model for externally loaded concentric-tube continuum robots," *IEEE Trans. Robot*, vol. 26, no. 5, pp. 769–780, 2010.

[13] A. Cohen, G. Zhang, F.-G. Tseng, U. Frodis, F. Mansfeld, and P. Will, "EFAB: rapid, low-cost desktop micromachining of high aspect ratio true 3-D MEMS ," in *IEEE Int. Conf. MEMS*, 1999.

[14] C. Bedell, J. Lock, A. Gosline, and P. Dupont, "Design optimization of concentric tube robots based on task and anatomical constraints," in *IEEE Int. Conf. on Robotics and Automation*, 2011, pp. 398 – 403.